

Accepted Manuscript

Synthesis and Biological evaluation of 2-(3,4-dimethoxyphenyl)-6-(2-[¹⁸F]fluoroethoxy) benzothiazole ([¹⁸F]FEDBT) for PET imaging of breast cancer

Geng-Ying Li, Daria D. Vaulina, Jia-Je Li, Olga S. Fedorova, Hsin-ElI Wang, Ren-Shyan Liu, Raisa N. Krasikova, Chuan-Lin Chen

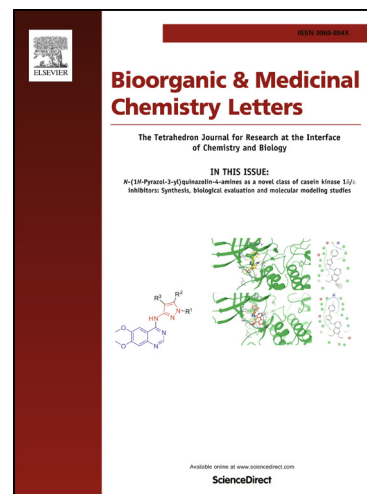
PII: S0960-894X(17)30577-2
DOI: <http://dx.doi.org/10.1016/j.bmcl.2017.05.079>
Reference: BMCL 25024

To appear in: *Bioorganic & Medicinal Chemistry Letters*

Received Date: 16 January 2017
Revised Date: 15 May 2017
Accepted Date: 26 May 2017

Please cite this article as: Li, G-Y., Vaulina, D.D., Li, J-J., Fedorova, O.S., Wang, H-E., Liu, R-S., Krasikova, R.N., Chen, C-L., Synthesis and Biological evaluation of 2-(3,4-dimethoxyphenyl)-6-(2-[¹⁸F]fluoroethoxy) benzothiazole ([¹⁸F]FEDBT) for PET imaging of breast cancer, *Bioorganic & Medicinal Chemistry Letters* (2017), doi: <http://dx.doi.org/10.1016/j.bmcl.2017.05.079>

This is a PDF file of an unedited manuscript that has been accepted for publication. As a service to our customers we are providing this early version of the manuscript. The manuscript will undergo copyediting, typesetting, and review of the resulting proof before it is published in its final form. Please note that during the production process errors may be discovered which could affect the content, and all legal disclaimers that apply to the journal pertain.



**Synthesis and Biological evaluation of
2-(3,4-dimethoxyphenyl)-6-(2-[¹⁸F]fluoroethoxy) benzothiazole ([¹⁸F]FEDBT) for
PET imaging of breast cancer**

Geng-Ying Li^{a,†}, Daria D. Vaulina^{b,†}, Jia-Je Li^a, Olga S. Fedorova^b, Hsin-Ell Wang^a,
Ren-Shyan Liu^{a,c,d}, Raisa N. Krasikova^{b,e*}, Chuan-Lin Chen^{a*}

^aDepartment of Biomedical Imaging and Radiological Sciences, National Yang-Ming University, Taipei, Taiwan

^bN.P. Bechtereva Institute of Human Brain, Russian Academy of Science, Saint-Petersburg, Russian Federation

^cMolecular and Genetic Imaging Core/Taiwan Mouse Clinic, National Comprehensive Mouse Phenotyping and Drug Testing Center, Taipei, Taiwan

^dNational PET/Cyclotron Center and Department of Nuclear Medicine, Taipei Veterans General Hospital, Taipei, Taiwan

^eSt.-Petersburg State University, Saint-Petersburg, Russian Federation

*Corresponding author:
Chuan-Lin Chen, Ph.D.
Tel: 886-2-28267062; Fax: 886-2-28201095
E-mail: clchen2@ym.edu.tw

*Corresponding author:
Raisa N. Krasikova, Ph.D.
Email: raisa@ihb.spb.ru

†These authors contributed equally to this work.

Abstract

Given the ever-present demand for improved PET radiotracer in oncology imaging, we have synthesized 2-(3,4-dimethoxyphenyl)-6-(2-[¹⁸F]fluoroethoxy)benzothiazole ([¹⁸F]FEDBT), a fluorine-18-containing fluoroethylated benzothiazole to explore its utility as a PET imaging tracer. [¹⁸F]FEDBT was prepared via kryptofix-mediated nucleophilic substitution of the tosyl group precursor. Fractionated ethanol-based solid-phase (SPE cartridge-based) purification afforded [¹⁸F]FEDBT in 60% radiochemical yield (EOB), with radiochemical purity in excess of 98% and the specific activity was 35 GBq/μmol. The radiotracer displayed clearly higher cellular uptake ratio in various breast cancer cell lines MCF7, MDA-MB-468 and MDA-MB-231. However, both biodistribution and microPET studies have showed a higher abdominal accumulation of [¹⁸F]FEDMBT and the tumor/muscle ratio of 1.8 was observed in the MDA-MB-231 xenograft tumors mice model. Further the lipophilic improvement is needed for the reduction of hepatobiliary accumulation and to promote the tumor uptake for PET imaging of breast cancer.

Breast cancer is the most prevalent malignancy and one of the major causes of cancer death in women worldwide. Approximately 15 to 20% of all breast cancer cases can be classified as triple-negative breast cancer (TNBC), characterized by the absence of gene expression for estrogen receptors (ERs), progesterone receptors (PRs) and human epidermal growth factor-2 (HER-2).¹⁻³ Clinical studies reveal that TNBC patients show significantly higher rates of recurrence at distant sites and poor prognosis.⁴ Therefore, early detection and molecular typing of breast cancer is essential for improving efficacy of therapeutic interventions and increasing survival rates.⁵ Mammography is a major tool for screening and early detection of breast cancer, however, its sensitivity is limited and frequent false positive diagnoses are a problem. Compared to standard X-ray mammography, positron emission tomography (PET), especially hybrid PET-CT imaging, can be used not only to detect cancer, but also to stage it, determine metabolic properties and biological status of the tumor, as well as help with the therapeutic response evaluation.⁶⁻⁸

Recently, versatile 2-arylbenzothiazole scaffold based compounds with high potential for diagnostic and therapeutic applications have been developed (Fig. 1).⁹⁻¹⁰ Carbon-11 labeled benzothiazole aniline (BTA) derivative, known as [¹¹C]PIB or Pittsburgh compound-B, demonstrated good binding properties towards A β plaques and excellent pharmacokinetics for imaging brain amyloid in Alzheimer's disease.¹¹ The corresponding ¹⁸F-labeled analogue known as [¹⁸F]flutemetamol (Vizamyl)¹² with similar diagnostic properties and benefits of longer half-life of fluorine-18 was approved for clinical PET application by FDA in 2013. As a matter of interest, a series of compounds based on 2-arylbenzothiazole described by Westwell et al. were found to inhibit tyrosine kinase.^{13,14} The lead compound of the library - 5-fluoro-2-(3,4-dimethoxyphenyl)benzothiazole (PMX-610) has demonstrated very potent (GI₅₀ < 0.1 nM for MCF-7 and MDA-468 cell lines) and selective *in vitro* antiproliferative properties for human lung, colon and breast cancer cell lines.¹⁴ Proposed mechanisms are based on the selective high affinity of aryl hydrocarbon Receptor (AhR) which act as both inducers and substrates for P450s 1A1 and 2W1. The PMX-610 forms activated AhR complexes which translocate to the nucleus inducing cyp1a1 gene transcription and expression of P450s 1A1 and 2W1 enzyme. The oxidation products of PMX-610 can form GSH conjugates which may lead to their possible toxicological consequences and result in formation of DNA adducts and ultimately cell death.¹⁵⁻¹⁷ Recently, Hiyoshi and co-workers also found a novel benzothiazole analogue, 2-(4-hydroxy-3-methoxyphenyl)benzothiazole (YL-109), with ability to inhibit TNBC cell growth and induce CHIP (C-terminus of Hsp70-Interacting Protein) transcription through AhR signaling in MDA-MB-231 cells.¹⁸ AhR overexpression and its activation are considered to be markers that predict

sensitivity of breast cancer cells to benzothiazole treatment. Therefore, development of new PET imaging probes to evaluate response of tumors to benzothiazole-based drugs is of significant importance. To date, only a handful of such PET and SPECT radiotracers have been reported. The [^{11}C]PMX-610 and other carbon-11 labeled 2-arylbenzothiazole analogues have been prepared via standard O - ^{11}C -methylation, but their potential as PET imaging agents needs to be further evaluated.¹⁹ The technecium-99m labeled complexes of 2-(4'-aminophenyl)benzothiazole II-A and II-B (Fig. 1) were developed by Pelecanou and co-workers as promising radiotracers for SPECT imaging of breast cancer.^{20,21} In biodistribution studies the tumor/muscle ratio of 2.2 for the most active complex II-B was observed using MCF-7 tumor bearing SCID mice, indicating suitability of benzothiazole scaffold for the development of radiopharmaceuticals.

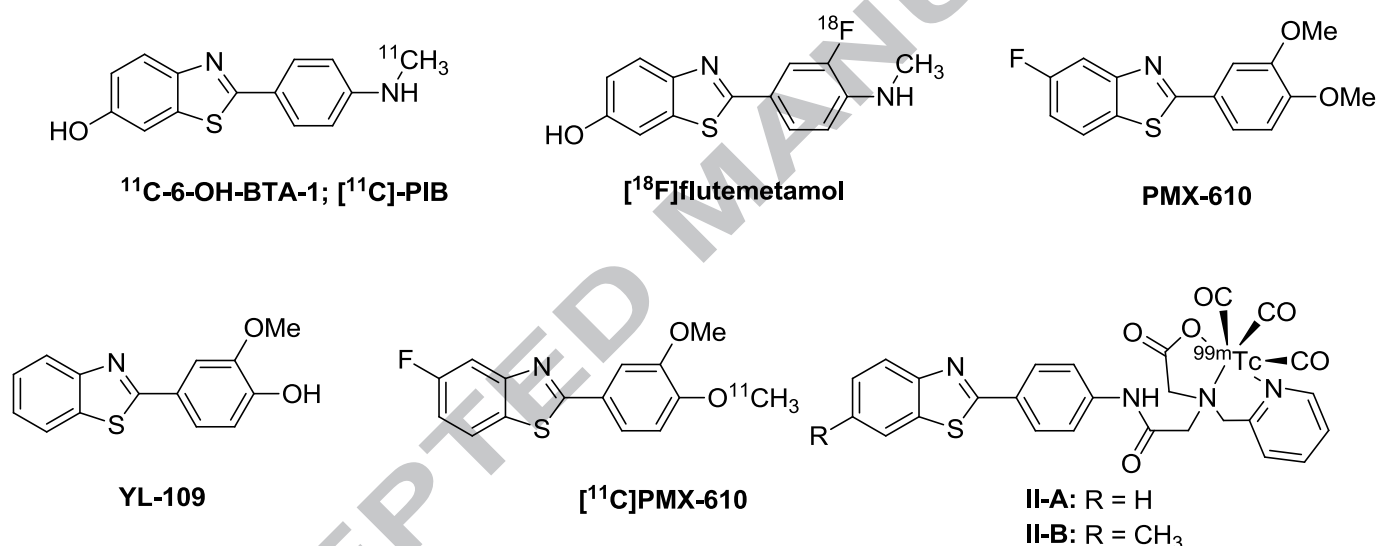


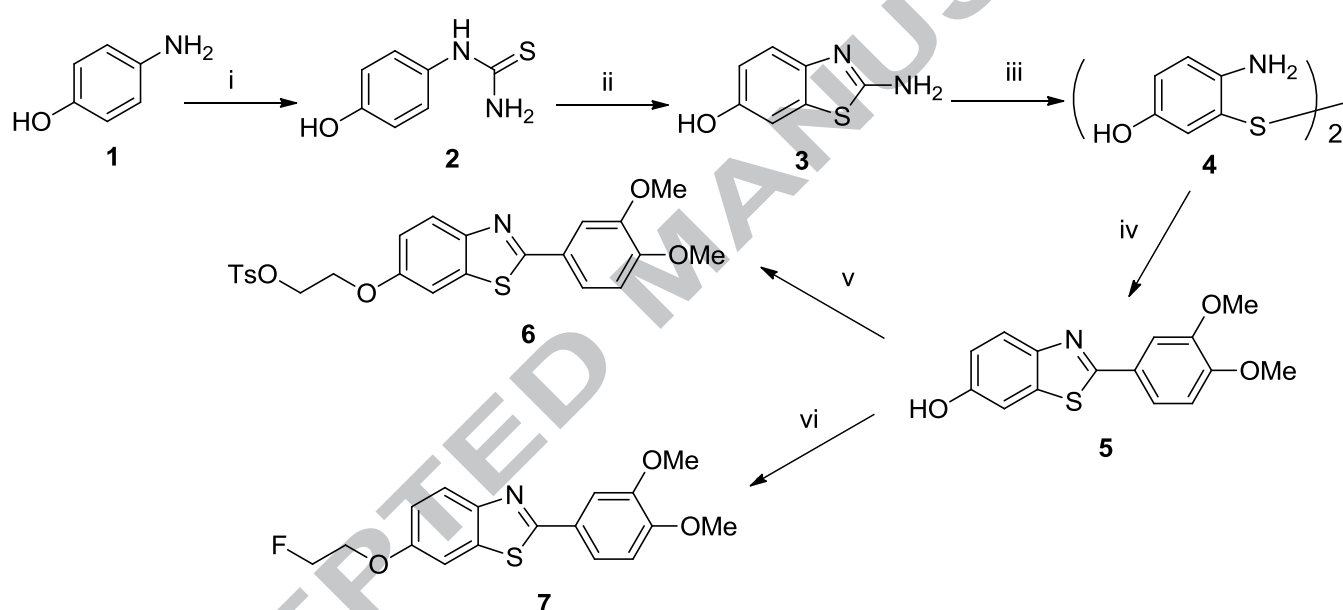
Figure 1. Chemical structures of the diagnostic or therapeutic 2-arylbenzothiazoles

To translate chemotherapeutic compound into diagnostic application in PET imaging, we have taken aim at developing a fluorine-18 labeled derivative of PMX-610, 2-(3,4-dimethoxyphenyl)-6-(2- ^{18}F fluoroethoxy)benzothiazole (^{18}F FEDBT). Introduction of ^{18}F -label into alkyl chain can be easily achieved via an $\text{S}_{\text{N}}2$ substitution reaction of tosylate in an appropriate precursor with an activated [^{18}F]fluoride.

We further report the results of an *in vitro* assessment of [^{18}F]FEDBT properties using MCF-7, MDA-MB-468 and MDA-MB-231 breast cancer cell lines as well as results of *in vivo* studies with MDA-MB-231 breast tumor bearing mice evaluating the potential of this benzothiazole derivative as breast cancer PET imaging agent.

The standard compound **7** and precursor **6** were synthesized in five steps following previously published methods with minor modification from the

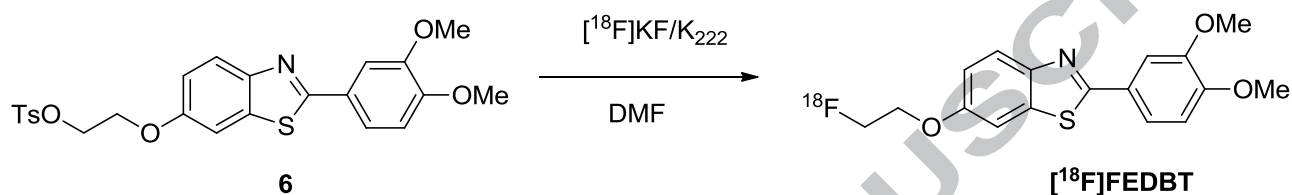
commercially available 4-hydroxyaniline as it is presented on the Scheme 1.^{19,22} Briefly, the aryl thiourea **2** was synthesized via condensation of 4-hydroxyaniline and potassium thiocyanate. The 2-amino-6-hydroxybenzothiazole **3** was obtained from the oxidative cyclization of compound **2** with bromine, followed by one-pot reaction of **3** with aqueous potassium hydroxide, followed by reaction with 3,4-dimethoxybenzaldehyde and triphenylphosphine with catalytic amount *p*-toluenesulfonic acid to obtain compound **5** - 6-hydroxy-2-(3,4-dimethoxyphenyl)benzothiazole in 36% yield. The precursor **6** and standard compound **7** were prepared from compound **5** via the direct alkylation with either ethylene glycol ditosylate or 2-fluoroethyl tosylate in 64% and 71% yield respectively.



Scheme 1. Synthesis of the labeling precursor **6** and authentic standard **7**: (i) 4-hydroxyaniline, KSCN, HCl, reflux 4h; (ii) Br₂, chloroform, reflux 4h; (iii) KOH, H₂O, ethylene glycol, reflux 12h; (iv) 3,4-dimethoxybenzaldehyde, *p*-toluene sulfonic acid, PPh₃, Toluene, reflux 15h; (v) ethylene di(*p*-toluenesulfonate), potassium carbonate, CH₃CN, reflux 12h; (vi) 1-fluoro-2-tosyloxyethane, potassium carbonate, CH₃CN, reflux 12h.

Radiosynthesis of the [¹⁸F]FEDBT was accomplished via Kryptofix-mediated nucleophilic substitution of the tosyl group in the precursor **6** with no-carrier-added (NCA) [¹⁸F]fluoride (Scheme 2) according to current state of the art.^{23,24} Fluorination was performed in anhydrous DMF at 140°C with 5 min reaction time; radiochemical conversion (RCC) was 90±3%, n=10, as determined by radioTLC analysis of the reaction mixture diluted by an aqueous ethanol. Fractional ethanol-based solid-phase

(SPE cartridge-based on tC18) purification afforded the product with 60% radiochemical yield (EOB) and radiochemical purity in excess of 98% . (Figure S1, S2 and Table S1). The identity of [^{18}F]FEDBT was confirmed by HPLC by co-injection with authentic reference **7** (Figure S2) and the specific activity was 35 GBq/ μmol (Figure S3 and S4). For *in vitro* stability evaluation the radiotracer was incubated at 37°C in FBS and PBS. In both buffers radiochemical purity of [^{18}F]FEDBT was higher than 80% after 120 min of incubation (Figure S5). The partition coefficient ($\log P$) of [^{18}F]FEDBT was determined to be 1.36 ± 0.11 ($n=3$).



Scheme 2. One-step radiosynthesis of [^{18}F]FEDBT using precursor **6**.

In *in vitro* cellular uptake studies [^{18}F]FEDBT was evaluated in MDA-MB-468, MCF-7 and MDA-MB-231 breast cancer cell lines. The results are presented in Fig. 4. Significant uptake of the radiotracer was observed already after 2 min incubation followed by gradual increase until reaching plateau after ca. 60 min. The percentage of total radioactivity observed was 11.4 ± 0.3 , 10.0 ± 0.2 and 9.1 ± 0.3 (% ID/ 10^5 cells) in MDA-MB-468, MCF-7 and MDA-MB-231 breast cancer cell lines respectively.

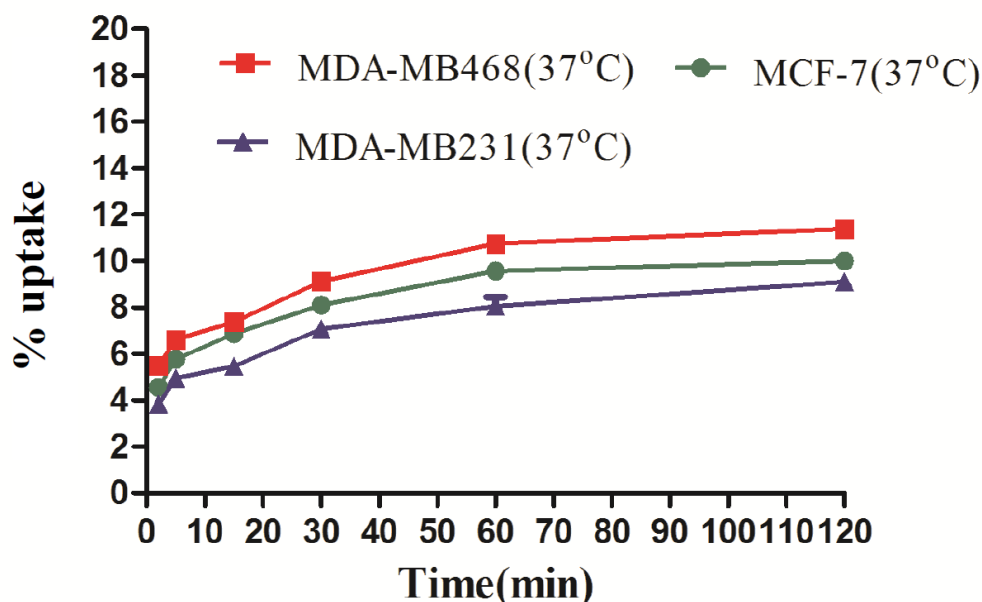


Figure 2. In vitro cellular uptake of [^{18}F]FEDBT in MCF-7, MDA-MB-468 and MDA-MB-231 breast cancer cells lines over time ($n = 5$; mean \pm SD).

The biodistribution of [^{18}F]FEDBT was investigated in the immune competent female NOD/SCID mice bearing MDA-MB-231 xenografts at different time points (15 min, 30 min, 1 h and 2 h) after intravenous injection of 3.7 MBq of radiotracer (Table 1). Biodistribution data indicates that [^{18}F]FEDBT has relatively slow blood and tumor clearance with moderate rate of excretion. Low retention of radioactivity was observed in non-target tissues, with the exception of the excretory system organs i.e. intestine, liver and kidney. These results indicate that the tracer undergoes both hepatobiliary and urinary excretion. The substantial radioactivity accumulation in bone tissue indicates that defluorination of the [^{18}F]FEDBT is occurring as well. Tumor uptake was 2.23 ± 0.35 % ID/g at 15 min and 2.47 ± 0.18 % ID/g at 60 min with the highest T/M ratio of 1.82 ± 0.25 at 120 min p.i (n=3).

Table 1. Biodistribution of [^{18}F]FEDBT in MDA-MB-231 tumor bearing mice at different time points after i.v. The results were expressed in % ID/g (n = 4; mean \pm SD); S.I: small intestine, L.I: large intestine.

Organ	15 min	30 min	60 min	120 min
Blood	2.68 \pm 0.23	2.49 \pm 0.17	2.37 \pm 0.17	2.74 \pm 0.13
Heart	2.33 \pm 0.28	1.91 \pm 0.02	1.80 \pm 0.16	1.87 \pm 0.47
Lung	2.29 \pm 0.28	1.77 \pm 0.16	1.71 \pm 0.19	1.30 \pm 0.28
Liver	3.41 \pm 0.29	2.32 \pm 0.18	2.07 \pm 0.18	4.30 \pm 1.84
Stomach	1.72 \pm 0.20	1.36 \pm 0.16	1.13 \pm 0.06	1.43 \pm 0.37
S.I.	6.07 \pm 2.76	2.73 \pm 0.41	1.94 \pm 0.28	1.67 \pm 0.34
L.I.	2.24 \pm 0.12	1.94 \pm 0.44	1.86 \pm 0.17	2.09 \pm 0.52
Pancreas	1.97 \pm 0.19	1.34 \pm 0.20	1.31 \pm 0.23	1.32 \pm 0.13
Spleen	2.10 \pm 0.05	1.52 \pm 0.12	1.49 \pm 0.14	2.71 \pm 0.98
Ovaries	2.94 \pm 0.79	2.15 \pm 0.12	2.26 \pm 0.19	2.03 \pm 0.27
Uterus	2.44 \pm 0.36	1.97 \pm 0.26	2.20 \pm 0.65	2.11 \pm 0.11
Muscle	1.84 \pm 0.16	1.66 \pm 0.27	1.64 \pm 0.16	1.37 \pm 0.11
Bone	3.27 \pm 0.64	5.66 \pm 0.62	5.11 \pm 1.06	3.01 \pm 2.26
Marrow	2.11 \pm 0.28	1.85 \pm 0.25	1.62 \pm 0.27	2.84 \pm 1.21
Bladder	2.55 \pm 0.32	1.78 \pm 0.27	2.04 \pm 0.91	2.53 \pm 0.49
Kidney	3.20 \pm 0.11	2.12 \pm 0.21	1.95 \pm 0.17	2.01 \pm 0.27
Feces	1.62 \pm 0.32	2.39 \pm 0.34	1.82 \pm 0.71	2.53 \pm 1.59
Brain	2.99 \pm 0.35	2.14 \pm 0.16	1.82 \pm 0.21	2.21 \pm 0.53
Tumor	2.23 \pm 0.35	2.73 \pm 0.36	2.46 \pm 0.26	2.47 \pm 0.18
T/B	0.83	1.10	1.03	0.90
T/M	1.27	1.64	1.50	1.80

The microPET images of the MDA-MB-231 tumor xenograft-bearing mice were recorded following bolus injection of 2-4 MBq of the [^{18}F]FEDBT in 200 μL of normal saline/10% DMSO into the lateral tail vein. Rapid radioactivity accumulation in the urinary bladder and abdomen indicated that [^{18}F]FEDBT was excreted mainly through renal and hepatobiliary pathways. The uptake in MDA-MB-231 xenografts was

observed at 60 min p.i. (Fig. 3) and could be delineated with appreciable tumor-to-background contrast within 120 min post-injection (Fig. S4). These results are consistent with the data from the biodistribution study.

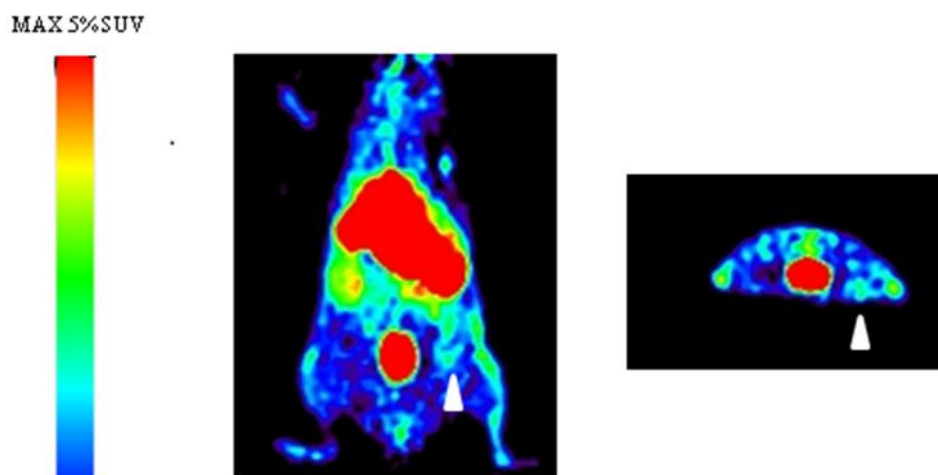


Figure 3. Representative coronal (left) and transaxial (right) [^{18}F]FEDBT microPET images of MDA-MB231 breast cancer-bearing mice. The microPET imaging was performed at 60 min p.i. of approximately 1.85 MBq of [^{18}F]FEDBT. Arrows head indicate tumors.

In summary, we have reported a one-step nucleophilic synthesis of [^{18}F]FEDBT with Sep-Pak purification procedure, with high (>60% EOB) radiochemical yield and excellent chemical and radiochemical purity in excess of 98%. The radiotracer revealed the significant high uptake in MCF7, MDA-MB-468 and MDA-MB-231 breast cancer cell lines. However, the lipophilicity of [^{18}F]FEDBT showed a higher hepatobiliary accumulation and lower tumor/muscle ratio was 1.8 in MDA-MB-231 tumor xenografts bearing mice. The results limited the utility of [^{18}F]FEDBT as a PET tracer for breast cancer imaging.

Acknowledgements: This study was supported by the Russian Foundation of Basic Research, RFBR grant 15-54-52026/16, MOST 104- 2923-B-010-001-MY2 and MOST 105-2314-B-010-035, Taiwan. We also thank the staff of National PET and Cyclotron Center in Taipei Veterans General Hospital, who kindly provided excellent technical assistance. Molecular and Genetic Imaging Core/Taiwan Mouse Clinic, National Comprehensive Mouse Phenotyping and Drug Testing Center, Taipei, Taiwan, is also gratefully acknowledged.

References:

1. Torre, L. A.; Bray, F.; Siegel, R. L.; Ferlay, J.; Lortet-Tieulent, J.; Jemal, A. *CA Cancer J. Clin.* **2015**, *65*, 87.
2. Foulkes, W. D.; Smith, I. E.; Reis-Filho, J. S. *N. Engl. J. Med.* **2010**, *363*, 1938.
3. Carey, L.; Winer, E.; Viale, G.; Cameron, D.; Gianni, L. *Nat. Rev. Clin. Oncol.* **2010**, *7*, 683.
4. Dent, R.; Trudeau, M.; Pritchard, K. I.; Hanna, W. M.; Kahn, H. K.; Sawka, C. A.; Lickley, L. A.; Rawlinson, E.; Sun, P.; Narod, S. A. *Clin. Cancer Res.* **2007**, *13*, 4429.
5. Tsujikawa, T.; Yoshida, Y.; Maeda, H.; Tsuchida, T.; Mori, T.; Kiyono, Y.; Kimura, H.; Okazawa, H. *Brit. J. Radiol.* **2012**, *85*, 1020.
6. Linden, H. M.; Dehdashti, F. *Semin. Nucl. Med.* **2013**, *43*, 324.
7. Oude Munnink, T.O.; Nagengast, W. B.; Brouwers, A. H.; Schröder, C. P.; Hospers, G. A Lub-de Hooge, M. N.; van der Wall, E.; van Diest, P. J.; de Vries, E. G. *The Breast*, **2009**, *18*, S66.
8. van Kruchten, M.; de Vries, E. G.; Brown, M.; de Vries, E. F.; Glaudemans, A. W.; Dierckx, R. A.; Schröder, C. P.; Hospers, G. A. *Lancet Oncol.* **2013**, *14*, e465.
9. Ono, M. *Chem. Pharm. Bull.* **2009**, *57*, 1029.
10. Henriksen, G.; Yousefi, B. H.; Drzezga, A.; Wester, H.J. *Eur J Nucl Med Mol Imaging.* **2008**, *35 (suppl. 1)*, S75.
11. Mathis, C.A.; Bacskai, B.J.; Kajdasz, S.T.; McLellan, M.E.; Frosch, M.P.; Hyman, B.T., Holt, D.P.; Wang, Y.; Huang, G-F.; Debnath, M.L.; Klunk, W.E. *Bioorg Med Chem Lett.* **2002**, *12*, 295.
12. Thal, D.R.; Beach, T.G., Zanette, M.; Hurling, K.; Chakrabarty, A.; Ismail, A.; Smith, A.P.L.; Buckley, C. *Alzheimer's & Dementia.* **2015**, *11*, 975.
13. Mortimer, C. G.; Wells, G.; Crochard, J.-P.; Stone, E. L.; Bradshaw, T. D.; Stevens, M. F. G.; Westwell, A. D. *J. Med. Chem.* **2006**, *49*, 179.
14. Aiello, S.; Wells, G.; Stone, E. L.; Kadri, H.; Bazzi, R.; Bell, D. R.; Stevens, M. F. G.; Matthews, C. S.; Bradshaw, T. D.; Westwell, A. D. *J. Med. Chem.* **2008**, *51*, 5135.
15. Tan, B.S.; Tiong, K.H.; Muruhadas, A.; Randhawa, N.; Choo, H.L.; Bradshaw, T.D.; Stevens, M.F.; Leong, C.O. *Mol Cancer Ther.* **2011**, *10*, 1982.
16. Stone, E.L.; Citossi, F.; Singh, R.; Kaur, B.; Gaskell, M.; Farmer, P.B.; Monks, A.; Hose, C.; Stevens, M.F.; Leong, C.O.; Stocks, M.; Kellam, B.; Marlow, M.; Bradshaw, T.D. *Bioorg. Med. Chem.* **2015**, *23*, 6891.
17. Wang, K.; Guengerich, F.P.; *Chem Res Toxicol.* **2012**, *25*, 1740.
18. Hiyoshi, H.; Goto, N.; Tsuchiya, M.; Iida, K.; Nakajima, Y.; Hirata, N., Kanda Y.; Nagasawa, K.; Yanagisawa, J. *Sci. Rep.* **2014**, *18*, 7095.

19. Wang, M.; Gao, M.; Mock, B. H.; Miller, K. D.; Sledge, G. W.; Hutchins, G. D.; Zheng, Q. H. *Bioorg. Med. Chem.* **2006**, *14*, 8599.
20. Tzanopoulou, S.; Pirmettis, I.C.; Patsis, G.; Paravatou-Petsotas, M.; Livaniou, E.; Papadopoulos, M.; Pelecanou, M. *J. Med. Chem.* **2006**, *49*, 5408.
21. Tzanopoulou, S.; Sagnou, M.; Paravatou-Petsotas, M.; Gourni, E.; Loudos, G.; Xanthopoulos, S.; Lafkas, D.; Kiaris, H.; Varvarigou, A.; Pirmettis, I.C.; Papadopoulos, M.; Pelecanou, M. *J. Med. Chem.* **2010**, *53*, 4633.
22. Sharma, P.; Kumar, A.; Kumari, P.; Singh, J.; Kaushik, M. P. *Med. Chem. Res.* **2012**, *21*, 1136.
23. Cai, L.; Lu, S.; Pike, V.W. *Eur. J. Org. Chem.*, **2008**, 2853.
24. Krasikova, R. *Curr. Org. Chem.* **2013**, *17*, 2097.

